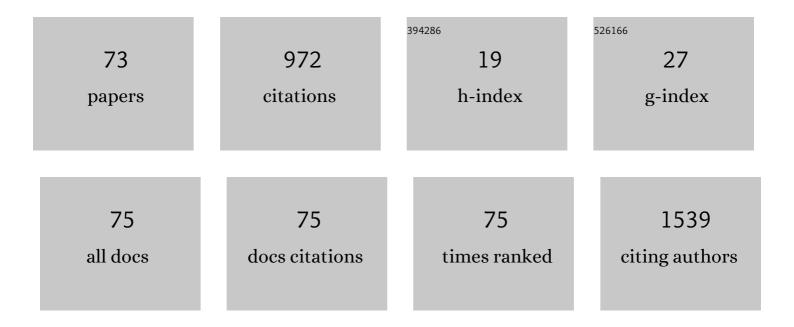
Zeng-Qiang Gao

List of Publications by Year in descending order

Source: https://exaly.com/author-pdf/6750454/publications.pdf Version: 2024-02-01



#	Article	IF	CITATIONS
1	Photonic Logic Gates Based on Control of FRET by a Solvatochromic Perylene Bisimide. Journal of Organic Chemistry, 2007, 72, 2878-2885.	1.7	76
2	Structure of the Type VI Effector-Immunity Complex (Tae4-Tai4) Provides Novel Insights into the Inhibition Mechanism of the Effector by Its Immunity Protein*. Journal of Biological Chemistry, 2013, 288, 5928-5939.	1.6	65
3	Synthesis, structures and magnetic properties in 3d-electron-rich isostructural complexes based on chains with sole syn–anti carboxylate bridges. Dalton Transactions, 2015, 44, 7213-7222.	1.6	46
4	Silver Ion-Mediated Heterometallic Three-Fold Interpenetrating Uranyl–Organic Framework. Inorganic Chemistry, 2015, 54, 10934-10945.	1.9	44
5	Exploring New Assembly Modes of Uranyl Terephthalate: Templated Syntheses and Structural Regulation of a Series of Rare 2D → 3D Polycatenated Frameworks. Inorganic Chemistry, 2017, 56, 7694-7706.	1.9	37
6	Supramolecular Host–Guest Inclusion for Distinguishing Cucurbit[7]urilâ€Based Pseudorotaxanes from Smallâ€Molecule Ligands in Coordination Assembly with a Uranyl Center. Chemistry - A European Journal, 2017, 23, 13995-14003.	1.7	33
7	Crystal and solution structures of methyltransferase RsmH provide basis for methylation of C1402 in 16S rRNA. Journal of Structural Biology, 2012, 179, 29-40.	1.3	31
8	Mononuclear copper(ii) complexes with 3,5-substituted-4-salicylidene-amino-3,5-dimethyl-1,2,4-triazole: synthesis, structure and potent inhibition of protein tyrosine phosphatases. Dalton Transactions, 2011, 40, 6532.	1.6	30
9	High-resolution structure of a new crystal form of BamA POTRA4–5 from <i>Escherichia coli</i> . Acta Crystallographica Section F: Structural Biology Communications, 2011, 67, 734-738.	0.7	30
10	Structural and Functional Characterization of Escherichia coli Toxin-Antitoxin Complex DinJ-YafQ. Journal of Biological Chemistry, 2014, 289, 21191-21202.	1.6	29
11	Novel Uranyl Coordination Polymers Based on Quinoline-Containing Dicarboxylate by Altering Auxiliary Ligands: From 1D Chain to 3D Framework. Crystal Growth and Design, 2016, 16, 4886-4896.	1.4	27
12	Structural insights into the inhibition of typeÂVI effector Tae3 by its immunity protein Tai3. Biochemical Journal, 2013, 454, 59-68.	1.7	26
13	Structure of the type VI secretion phospholipase effector Tle1 provides insight into its hydrolysis and membrane targeting. Acta Crystallographica Section D: Biological Crystallography, 2014, 70, 2175-2185.	2.5	26
14	Structure–function analyses reveal the molecular architecture and neutralization mechanism of a bacterial HEPN–MNT toxin–antitoxin system. Journal of Biological Chemistry, 2018, 293, 6812-6823.	1.6	24
15	Crystal structure of type VI effector Tse1 from <i>Pseudomonas aeruginosa</i> . FEBS Letters, 2012, 586, 3193-3199.	1.3	23
16	Structural Basis for Interaction between Mycobacterium smegmatis Ms6564, a TetR Family Master Regulator, and Its Target DNA. Journal of Biological Chemistry, 2013, 288, 23687-23695.	1.6	22
17	Structure–function studies of <i><scp>E</scp>scherichia coli</i> â€ <scp>RnlA</scp> reveal a novel toxin structure involved in bacteriophage resistance. Molecular Microbiology, 2013, 90, 956-965.	1.2	21
18	The crystal structure of the MPN domain from the COP9 signalosome subunit CSN6. FEBS Letters, 2012, 586, 1147-1153.	1.3	20

ZENG-QIANG GAO

#	Article	IF	CITATIONS
19	New Insight of Coordination and Extraction of Uranium(VI) with N-Donating Ligands in Room Temperature Ionic Liquids: <i>N</i> , <i>N</i> ′-Diethyl- <i>N</i> , <i>N</i> ′-ditolyldipicolinamide as a Case Study. Inorganic Chemistry, 2015, 54, 1992-1999.	1.9	20
20	Structural and SAXS analysis of the budding yeast SHU omplex proteins. FEBS Letters, 2012, 586, 2306-2312.	1.3	18
21	Structural insight into the E.Âcoli HigBA complex. Biochemical and Biophysical Research Communications, 2016, 478, 1521-1527.	1.0	17
22	Structural insights into the inhibition mechanism of bacterial toxin LsoA by bacteriophage antitoxin Dmd. Molecular Microbiology, 2016, 101, 757-769.	1.2	16
23	Structural characterizations of phage antitoxin Dmd and its interactions with bacterial toxin RnIA. Biochemical and Biophysical Research Communications, 2016, 472, 592-597.	1.0	16
24	Structural Insights Into the Transcriptional Regulation of HigBA Toxin–Antitoxin System by Antitoxin HigA in Pseudomonas aeruginosa. Frontiers in Microbiology, 2019, 10, 3158.	1.5	16
25	Crystal structures of multicopper oxidase CueO G304K mutant: structural basis of the increased laccase activity. Scientific Reports, 2018, 8, 14252.	1.6	15
26	The crystal structure of KSHV ORF57 reveals dimeric active sites important for protein stability and function. PLoS Pathogens, 2018, 14, e1007232.	2.1	15
27	Structural basis for the interaction of BamB with the POTRA3–4 domains of BamA. Acta Crystallographica Section D: Structural Biology, 2016, 72, 236-244.	1.1	14
28	Crystal structure and site-directed mutagenesis of a nitroalkane oxidase from Streptomyces ansochromogenes. Biochemical and Biophysical Research Communications, 2011, 405, 344-348.	1.0	13
29	Insights into the Catalytic Mechanism of 16S rRNA Methyltransferase RsmE (m3U1498) from Crystal and Solution Structures. Journal of Molecular Biology, 2012, 423, 576-589.	2.0	13
30	Conserved residues that modulate protein <i>trans</i> -splicing of <i>Npu</i> DnaE split intein. Biochemical Journal, 2014, 461, 247-255.	1.7	11
31	Insights into the Cross-Immunity Mechanism within Effector Families of Bacteria Type VI Secretion System from the Structure of StTae4-EcTai4 Complex. PLoS ONE, 2013, 8, e73782.	1.1	11
32	Genome-Wide Mapping of the Binding Sites and Structural Analysis of Kaposi's Sarcoma-Associated Herpesvirus Viral Interferon Regulatory Factor 2 Reveal that It Is a DNA-Binding Transcription Factor. Journal of Virology, 2016, 90, 1158-1168.	1.5	10
33	Structural analysis of Wss1 protein from saccharomyces cerevisiae. Scientific Reports, 2017, 7, 8270.	1.6	10
34	Structural analysis of <i>Pseudomonas aeruginosa</i> H3â€₹6SS immunity proteins. FEBS Letters, 2016, 590, 2787-2796.	1.3	9
35	Structure and Biochemical Characteristics of the Methyltransferase Domain of RNA Capping Enzyme from African Swine Fever Virus. Journal of Virology, 2021, 95, .	1.5	9
36	Structure of the putative dihydroorotate dehydrogenase from <i>Streptococcus mutans</i> . Acta Crystallographica Section F: Structural Biology Communications, 2011, 67, 182-187.	0.7	8

ZENG-QIANG GAO

#	Article	IF	CITATIONS
37	Structural and functional analysis show that the <i>Escherichia coli</i> uncharacterized protein <scp>Y</scp> jc <scp>S</scp> is likely an alkylsulfatase. Protein Science, 2014, 23, 1442-1450.	3.1	8
38	Structural Insights into the Methylation of C1402 in 16S rRNA by Methyltransferase Rsml. PLoS ONE, 2016, 11, e0163816.	1.1	8
39	Structure of orotate phosphoribosyltransferase from the caries pathogen <i>Streptococcus mutans</i> . Acta Crystallographica Section F: Structural Biology Communications, 2010, 66, 498-502.	0.7	7
40	Synthesis, Crystal Structure, and Characterization of the Charge-Transfer Salt (BEDT-TTF)[Fe(C2O4)Cl2](CH2Cl2), {BEDT-TTF = Bis(ethylenedithio)tetrathiafulvalene}. European Journal of Inorganic Chemistry, 2014, 2014, 4028-4032.	1.0	7
41	Conformational changes of antitoxin HigA from Escherichia coli str. K-12 upon binding of its cognate toxin HigB reveal a new regulation mechanism in toxin-antitoxin systems. Biochemical and Biophysical Research Communications, 2019, 514, 37-43.	1.0	7
42	Structural basis for recognition of the type VI spike protein VgrG3 by a cognate immunity protein. FEBS Letters, 2014, 588, 1891-1898.	1.3	6
43	Structural and SAXS analysis of Tle5–Tli5 complex reveals a novel inhibition mechanism of H2â€T6SS in <i>Pseudomonas aeruginosa</i> . Protein Science, 2017, 26, 2083-2091.	3.1	6
44	Structure analysis of the global metabolic regulator Crc from <i>Pseudomonas aeruginosa</i> . IUBMB Life, 2013, 65, 50-57.	1.5	5
45	NMR structure of the Nâ€terminalâ€most HRDC1 domain of RecQ helicase from <i>Deinococcus radiodurans</i> . FEBS Letters, 2013, 587, 2635-2642.	1.3	5
46	Crystal structures and kinetic properties of enoylâ€acyl carrier protein reductase I from <i>Candidatus Liberibacter asiaticus</i> . Protein Science, 2014, 23, 366-377.	3.1	5
47	Crystal structure of GnsA from Escherichia coli. Biochemical and Biophysical Research Communications, 2015, 462, 1-7.	1.0	5
48	Crystal structure of the putative cytoplasmic protein STM0279 (Hcp2) from <i>Salmonella typhimurium</i> . Acta Crystallographica Section F, Structural Biology Communications, 2017, 73, 463-468.	0.4	5
49	Mechanism of the allosteric regulation of <i>Streptococcus mutans</i> 2′-deoxycytidylate deaminase. Acta Crystallographica Section D: Structural Biology, 2016, 72, 883-891.	1.1	4
50	(BEDTâ€ITF) ₂ Cu ₂ (HCOO) ₅ : An Organic–Inorganic Hybrid Conducting Magnet. ChemistryOpen, 2017, 6, 320-324.	0.9	4
51	Structural and biochemical characterization of the yeast HD domain containing protein YGK1 reveals a metal-dependent nucleoside 5Ê ¹ -monophosphatase. Biochemical and Biophysical Research Communications, 2018, 501, 674-681.	1.0	4
52	The crystal structure of human protein α1M reveals a chromophore-binding site and two putative protein–protein interfaces. Biochemical and Biophysical Research Communications, 2013, 439, 346-350.	1.0	3
53	HicAB toxin–antitoxin complex fromEscherichia coli: expression and crystallization. Acta Crystallographica Section F, Structural Biology Communications, 2017, 73, 505-510.	0.4	3
54	Structural and functional characterization of the deep-sea thermophilic bacteriophage GVE2 tailspike protein. International Journal of Biological Macromolecules, 2020, 164, 4415-4422.	3.6	3

ZENG-QIANG GAO

#	Article	IF	CITATIONS
55	Characterization of the <i>Pseudomonas aeruginosa</i> T6SS PldB immunity proteins PA5086, PA5087 and PA5088 explains a novel stockpiling mechanism. Acta Crystallographica Section F, Structural Biology Communications, 2020, 76, 222-227.	0.4	3
56	Insights into the Neutralization and DNA Binding of Toxin–Antitoxin System ParESO-CopASO by Structure-Function Studies. Microorganisms, 2021, 9, 2506.	1.6	3
57	The 1.6Ã resolution structure of activated D138L mutant of catabolite gene activator protein with two cAMP bound in each monomer. International Journal of Biological Macromolecules, 2011, 48, 459-465.	3.6	2
58	The structural basis of the response regulator DrRRA from Deinococcus radiodurans. Biochemical and Biophysical Research Communications, 2012, 417, 1206-1212.	1.0	2
59	High-resolution crystal structure reveals a HEPN domain at the C-terminal region of S. cerevisiae RNA endonuclease Swt1. Biochemical and Biophysical Research Communications, 2014, 453, 826-832.	1.0	2
60	Oxovanadium(IV) Schiff Base Complex Derived From Phenylalanine Analogue Containing 2,3-Diaminopropionic Acid (DAP): Synthesis, Computational Study, and Biological Evaluation. Synthesis and Reactivity in Inorganic, Metal Organic, and Nano Metal Chemistry, 2015, 45, 455-467.	0.6	2
61	NUDIM: A non-uniform fast Fourier transform based dual-space constraint iterative reconstruction method in biological electron tomography. Journal of Structural Biology, 2021, 213, 107770.	1.3	2
62	Organic–inorganic hybrid metallic conductors based on bis(ethylenedithio)tetrathiafulvalene cations and antiferromagnetic oxalate-bridged copper(<scp>ii</scp>) dinuclear anions. Journal of Materials Chemistry C, 2022, 10, 2845-2852.	2.7	2
63	Structural insights into the function of 23S rRNA methyltransferase RlmG (m2G1835) from Escherichia coli. Rna, 2012, 18, 1500-1509.	1.6	1
64	Cloning, purification, crystallization and preliminary X-ray studies of human α1-microglobulin. Acta Crystallographica Section F: Structural Biology Communications, 2012, 68, 692-694.	0.7	1
65	Purification, crystallization and preliminary crystallographic analysis of the 23S rRNA methyltransferase RlmM (Cm2498) fromEscherichia coli. Acta Crystallographica Section F: Structural Biology Communications, 2013, 69, 640-642.	0.7	1
66	Application of a conic glass monocapillary in Beijing synchrotron radiation facility. Nuclear Instruments and Methods in Physics Research, Section A: Accelerators, Spectrometers, Detectors and Associated Equipment, 2014, 754, 42-45.	0.7	1
67	Cloning, purification, crystallization and preliminary X-ray studies of the putative type VI secretion immunity protein Tli5 (PA5088) fromPseudomonas aeruginosa. Acta Crystallographica Section F, Structural Biology Communications, 2014, 70, 903-905.	0.4	1
68	An iterative refinement method combining detector geometry optimization and diffraction model refinement in serial femtosecond crystallography. Radiation Detection Technology and Methods, 2018, 2, 1.	0.4	1
69	A noise and artifact suppression using resampling (NASR) method to facilitate de novo protein structure determination. Radiation Detection Technology and Methods, 2019, 3, 1.	0.4	1
70	Crystal structure of the type VI immunity protein Tdi1 (Atu4351) from <i>Agrobacterium tumefaciens</i> . Acta Crystallographica Section F, Structural Biology Communications, 2019, 75, 153-158.	0.4	1
71	Protein Preparation, Crystallization and Preliminary X-Ray Crystallographic Studies of Smu.1392c from Streptococcus mutans. Protein and Peptide Letters, 2006, 13, 1051-1052.	0.4	0

Synthesis, crystal structures and characterization of two heterometallic compounds: Ba 3 [Fe(C 2 O 4) Tj ETQq0 0 0 rgBT /Overlock 10 T 1.2 0 399-404.

5

#	Article	IF	CITATIONS
73	Crystal structure of the nucleoid-associated protein Fis (PA4853) from <i>Pseudomonas aeruginosa</i> . Acta Crystallographica Section F, Structural Biology Communications, 2020, 76, 209-215.	0.4	0